Metamaterial Enhanced Wireless Power Transfer For Underwater Robots Using Tri-Directional Coils

Akarsh Pokkunuru
Wichita State University, KS
axpokkunuru@shockers.wichita.edu

Hongzhi Guo
Univ. of Southern Maine, ME
hongzhi.guo@maine.edu

Xin Tan, Zhi Sun
Univ. at Buffalo, NY
xtan3, zhisun@buffalo.edu

Pu Wang
Univ. of North Carolina at Charlotte, NC
pu.wang@uncc.edu

***Abstract*—This paper demonstrates the metamaterial enhanced tri-directional coil wireless power transfer (WPT) solution for underwater robots. A tri-directional coil antenna is employed to enable multi-directional WPT and thereby greatly reducing the power loss in a scenario where the transmit-receive coil pairs are misaligned due to random orientation. Furthermore, the impact of parameters such as LOS distance, operating frequency, antenna depth, coil turns, and water conductivity are thoroughly analyzed subject to optimizing the power efficiency in a given environment. Through theoretical verification, we show that superior performance can be achieved using our antenna in contrast to conventional WPT techniques. Additionally, we also validate that operating near the water surface with a low frequency and fewer coil turns maximizes the overall reliability of power transfer in lossy water environments.**

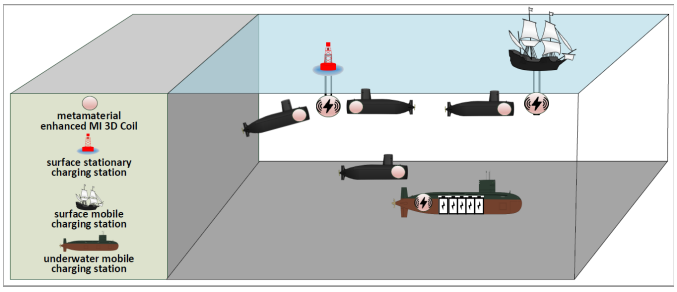

Fig. 1: Overall system architecture of underwater wireless power transfer

I. Introduction

Around 95% of the oceans and lakes are uncharted territories in our planet. Scientists and researchers across the globe are working tirelessly on this subject as there is an immense scope for accomplishing future advancements. A major chunk of these ocean based applications are being accomplished through the assistance of autonomous underwater vehicles (AUV) and remotely operated underwater vehicles (ROV). As a result, underwater robotics based applications are a popular solution nowadays not only in exploration [1] but, they are also becoming highly relevant in applications such as maritime surveillance, geohazard and pollution monitoring [2], [3], [4] or just as a recreational hobby due to the added convenience of small size, high mobility and some other nifty features accomplished with the help of sensors and cameras.

Despite the benefits, the runtime of these rovers is considerably meagre, and it is essential to supply power on a regular basis. Further, the hassle of safely recovering the rover from water, replenishing its battery and recommissioning it back, is an extremely unattractive and inconvenient solution. Therefore, solving this challenge was one of our main catalysts behind this paper. Apart from hassle free charging via magnetic coupling, another quirk we intend to address in this paper, is the concern of maintaining tight alignment between the transmit-receive coils during power transmission. In literature, conventional WPT through the use of uni-directional or resonating coils has been demonstrated in [5] to [11]. The advantage of these solutions is that the system is relatively easy to design however, the range of charging and the requirement of tight alignment during power transmission is a necessity to achieve best performance. Thus, we address these issues through the use of our metamaterial enhanced tri-directional coil antenna [12], [13]. The metamaterial shell in our antenna works in resonance with the engulfed coil antenna thus enhancing the charging range and thereby establishing a reasonable coupling factor between TX-RX pair. Additionally, the tri-directional coil can capture the magnetic fields propagating along the direct, reflected, and the lateral waves due to additional degrees of freedom (DOF) compared to a uni-directional coil antenna. Hence, with these design improvements, the need for tight alignment between Tx-Rx can be relaxed and likewise, we can achieve higher efficiencies in power transfer.

The entirety of this paper is categorized as follows: in Section II, we introduce a mathematical model for wireless power transfer system and its corresponding power transfer efficiency is derived. Then in Section III, we focus on the underwater channel and its impact on mutual inductance between the TX-RX. In Section IV, we validate our proof of concept via simulations results and Section V concludes our paper.

II. Power Transfer Modeling

In an occasion where the AUV runs out of power, it is scheduled to return to the charging base stations as seen in Fig. (1). Here, both the base station and the AUV are equipped with a similar antenna setup which consists of a tri-directional coil antenna engulfed by a metamaterial shell. The actual implementation of this antenna can be viewed in Fig. (2) below. Once the AUV is within the vicinity of the base station, it begins to recharge its batteries. Assuming this simple

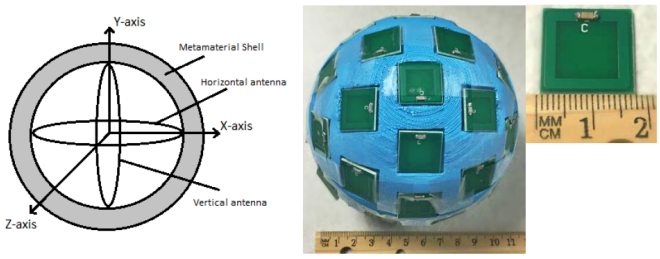

Fig. 2: Internal and outer shell view of the Metamaterial enhanced Tri-directional coil antenna [12]

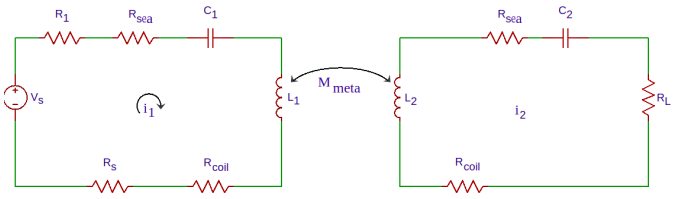

Fig. 3: Wireless Power Transfer Circuit Model

scenario, we provide comprehensive theoretical insights into the power transfer efficiency, which is the ratio of received power across the load resistor R_L and the transmitted power from equ. (17). The power transfer efficiency in turn depends on our underwater channel model [13], [14] due to the mutual inductance between TX-RX coils. The antenna setup can be visualized with an equivalent RLC circuit model as shown in Fig. (3). Power efficiency is analyzed in two mediums of operation i.e.; lake and sea water environments ($0.1\,S/m$ and $4\,S/m$ respectively). In the transmit coil side, V_S is the voltage source from the charging base station and its corresponding voltage drop is modeled as R_S. The components R_1, L_i, C_i, $i = 1, 2$ are the resistance, capacitance and self-inductance equivalent to that of a circularly wound coil antenna. R_L is the load resistance due to the rover being charged at the charging station, R_{coil} is the resistance offered due to the conductive wire itself. M_{meta} is the mutual inductance between the transmitter and the receiver coil as a function of operating frequency, relative distance between Tx-Rx pair and the number of coil turns. A comprehensive description of M_{meta} will be provided in Section III, as its parameters strongly depend on the available channel conditions. As seen in Fig. (3), we initialize the derivation by applying Kirchhoff voltage law (KVL) to solve for the currents in both the TX-RX pair antennas. Through the course of this paper, frequency domain representation is used as the standard for notation. Hence, the KVL expression for transmit coil is given as follows:

$$-V_s + i_1\,R_S + i_1\,R_{coil} + i_1\,R_{sea} + i_1\,R_1 + i_1\,\frac{1}{j\omega C_1} + i_1\,j\omega L_1 - M_{meta}\,i_2 = 0 \quad (1)$$

here, V_s is the input AC voltage source, i_1 and i_2 are the currents in transmit and receive coils, R_S is the resistance due to the voltage drop, R_{coil} is the resistance offered by the coil and this expression is given as follows:

$$R_{coil} = \frac{2\,a\,N}{\rho_c\left(r_w^2 - (r_w - \sqrt{\frac{2}{\rho_c\,\omega\,\mu_0}})^2\right)} \quad (2)$$

where a is the coil radius, N is the number of coil turns, $\omega = 2\pi f$ where, f is the operating frequency, r_w wire radius, ρ_c is the conductivity of the wire and μ_0 is the permeability of free space. R_{sea} is the resistance offered by the water medium during transmission. Similarly, KVL across the receiving coil can be expressed as follows:

$$0 = i_2\,R_L + i_2\,R_{coil} + i_2\,R_{sea} + i_2\,\frac{1}{j\omega C_2} + i_2\,j\omega L_2 - M_{meta}\,i_1 \quad (3)$$

Rearranging the equations (1) and (3), we get:

$$i_1\left(R_S + R_{coil} + R_{sea} + R_1 + \frac{1}{j\omega C_1} + j\omega L_1\right) - M_{meta}\,i_2 = V_S \quad (4)$$

$$-M_{meta}\,i_1 + i_2\left(R_L + R_{coil} + R_{sea} + \frac{1}{j\omega C_2} + j\omega L_2\right) = 0 \quad (5)$$

Through simple algebraic manipulations, we can solve for i_1, i_2 in equations (4) and (5) which will yield us the currents across both the transmitter and receiver. Consequently, we can find the target voltage across the load resistor R_L as follows:

$$i_2 = \frac{M_{meta}\,i_1}{R_L + R_{coil} + R_{sea} + \frac{1}{j\omega C_2} + j\omega L_2} \quad (6)$$

Substituting (6) into (4) and rearranging the terms yields i_1, which is given as follows:

$$i_1 = \frac{V_s}{\alpha_1 - \beta_1} \quad (7)$$

$$\alpha_1 = \left(R_S + R_{coil} + R_{sea} + R_1 + \frac{1}{j\omega C_1} + j\omega L_1\right) \quad (8)$$

where α_1 and β_1 are given as follows:

$$\beta_1 = \frac{M_{meta}^2}{R_L + R_{coil} + R_{sea} + \frac{1}{j\omega C_2} + j\omega L_2} \quad (9)$$

We can solve equation (6) by substituting (7) in (6) and rearrange some terms which is given as follows:

$$i_2 = \frac{M_{meta}\,V_S}{\alpha_2 - \beta_2} \quad (10)$$

where α_2 and β_2 are given as follows:

$$\alpha_2 = \left(R_S + R_{coil} + R_{sea} + R_1 + \frac{1}{j\omega C_1} + j\omega L_1\right) \quad (11)$$

$$\beta_2 = \left(R_L + R_{coil} + R_{sea} + \frac{1}{j\omega C_2} + j\omega L_2\right) - M_{meta}^2 \quad (12)$$

Now, we will work towards obtaining the target voltage across the load resistor R_L at receiver, which will yield us

the amount of power which was successfully transferred from the transmitter. This is given by Ohm's law as follows:

$$V_{R_L} = i_2 \, R_L \tag{13}$$

Further, the voltage ratio equation after substituting (10) in (13) and rearranging terms will yield us the following equation:

$$\frac{V_{R_L}}{V_S} = \frac{M_{meta} \, R_L}{\delta_1 \, \delta_2 - M_{meta}^2} \tag{14}$$

where δ_1 and δ_2 are given as:

$$\delta_1 = \left(R_S + R_{coil} + R_{sea} + R_1 + \frac{1}{j\omega C_1} + j\omega L_1\right) \tag{15}$$

$$\delta_2 = \left(R_L + R_{coil} + R_{sea} + \frac{1}{j\omega C_2} + j\omega L_2\right) \tag{16}$$

Finally, the power ratio or the wireless power transfer efficiency is the ratio of received power across R_L and the transmitted power, which is given by the following equation:

$$\eta = \frac{P_{R_L}}{P_{in}} = \frac{i_2 \, V_{R_L}}{i_1 \, V_S} \tag{17}$$

where i_1, i_2 are given from equ. (7) and (10), V_S is the voltage across power source and V_{R_L} is the measured voltage across the load R_L.

III. Mutual Inductance and Channel Model Considerations

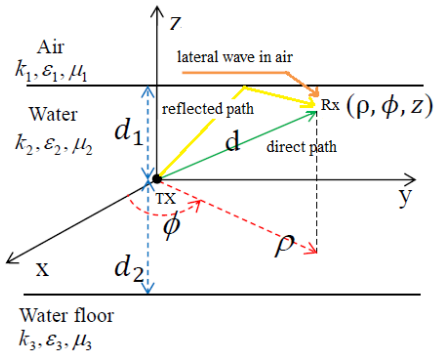

Fig. 4: Tx as a charging base station and Rx as a robot to be charged

IV. Mutual Inductance and Channel Model Considerations

In the prior section, we derived the wireless power transfer efficiency in equ. (17) which is apparently a function of the metamaterial enhanced mutual induction M_{meta}. In this section, we describe the impact of underwater environment on mutual inductance which is a function of coil orientation and underwater MI channel conditions. As seen in Fig. (4), the transmit-receive pairs are assumed to be in a shallow water environment where *TX* and *RX* depicts the charging base station and rover locations respectively. The direct line-of-sight (LOS) distance between TX-RX is denoted by d. Similarly,

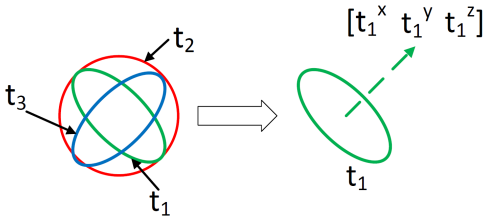

Fig. 5: Transmitter and Receiver Coil orientation

the vertical distance from the water surface to *TX* is denoted by d_1 and the corresponding distance from the water bed is noted by d_2. The random orientation of the *TX-RX* antennas is considered in 3D Cartesian space as shown below.

$$\mathbf{T} = \begin{bmatrix} t_1^x & t_1^y & t_1^z \\ t_2^x & t_2^y & t_2^z \\ t_3^x & t_3^y & t_3^z \end{bmatrix} \tag{18}$$

$$\mathbf{R} = \begin{bmatrix} r_1^x & r_1^y & r_1^z \\ r_2^x & r_2^y & r_2^z \\ r_3^x & r_3^y & r_3^z \end{bmatrix} \tag{19}$$

here each row in the matrices is an unit vector, which indicates the direction of each coil in 3D space. For example, the orientation of the transmitting coil t_1 is shown in Fig. (5). If we treat the transmitter and receiver coils as 3×3 MIMO system, we can obtain a 3×3 magnetic field strength matrix in equ. (20) by following our underwater MI channel model [13]. Each element in this matrix is the received magnetic field strength at the receiver coil RX_r, $(r = 1, 2, 3)$, contributed by a particular transmitter coil TX_t, $(t = 1, 2, 3)$. The received magnetic field strength includes the components propagating along the direct path, reflected path and the lateral waves. The parameters in equ. (20) are illustrated in Fig. (4). In particular I_0, I_x and I_y are the unit currents passing through each unidirectional coil antennas and N, a are the number of coil turns and coil radius respectively. Also, k_i, μ_i and ϵ_i, $i = 1, 2$ are the propagation constant, permeability, and permittivity in air and water respectively. Based on magnetic field matrix from equ. (20), we can find the mutual inductance [13] between the transmitter and receiver coils as follows:

$$M_{tri} = \phi_r \, \mathbf{I}_c^{-1} = \mu_0 \, \pi \, a^2 \, N \, \mathbf{R} \, \mathbf{L}_t \, \mathbf{H}_{cl}(w, d) \, \mathbf{T}^T \tag{21}$$

here, ϕ_r is the magnetic flux in the receiving coil and $\mathbf{I}_c$ is the current along the each unidirectional coil inside the metamaterial shell. Additionally, the mutual inductance can also be expressed in terms of its magnetic field strength as shown in (21). Here, $\mathbf{L_t}$ is the cylindrical to Cartesian coordinate conversion matrix given below in (22) and T, R are given from equ. (18) and (19) are the transmit-receive coil orientations respectively.

$$\mathbf{L_t} = \begin{bmatrix} cos\phi & -sin\phi & 0 \\ sin\phi & cos\phi & 0 \\ 0 & 0 & 1 \end{bmatrix} \tag{22}$$

The expression given in (21) accounts to the effects observed in the tri-directional coil along all the paths (direct,

$$H_{cl}(\omega,d)=\begin{pmatrix} -\frac{j\,I_x\,N\,a^2\,k_1\,e^{j\,d\,k_1+2j\,d_1\,k_2-j\,k_2\,z_r}\,\cos(\phi_x)}{2\,d^2} & -\frac{j\,I_y\,N\,a^2\,k_1\,e^{j\,d\,k_1+2j\,d_1\,k_2-jk_2\,z_r}\,\cos(\phi_y)}{2\,d^2} & \frac{I_0\,N\,a^2\,k_2{}^2\,e^{j\,d\,k_2}}{4\,d^2} \\ \frac{I_x\,N\,a^2\,e^{j\,d\,k_1+2jd_1\,k_2-jk_2\,z_r}\,\sin(\phi_x)}{2\,d^3} & \frac{I_y\,N\,a^2\,e^{j\,d\,k_1+2jd_1\,k_2-jk_2\,z_r}\,\sin(\phi_y)}{2\,d^3} & 0 \\ -\frac{jI_x\,N\,a^2\,k_1{}^2\,e^{j\,d\,k_1+2jd_1\,k_2-jk_2\,z_r}\,\cos(\phi_x)}{2\,d^2\,k_2} & -\frac{jI_y\,N\,a^2\,k_1{}^2\,e^{j\,d\,k_1+2jd_1\,k_2-jk_2\,z_r}\,\cos(\phi_y)}{2\,d^2\,k_2} & -\frac{I_0\,N\,a^2\,k_2\,e^{j\,d\,k_2}}{4\,d} \end{pmatrix} \quad (20)$$

reflected and lateral). The enhancement due to the metamaterial shell is also necessary to be modeled as tri-directional coil is enclosed by the metamaterial shell. Mathematically, the enhancement is achieved by matching the negative μ metamaterials with the positive μ environment, which creates a resonant status for the entire antenna structure. By using the spherical vector wave functions with boundary conditions, we can calculate the magnetic field distribution at receiver side and derive the mutual induction by following our previous research [14]. However, such method is quite involving. Thus, in this paper, we approximate M_meta by our field experiments [12] as follows:

$$M_{meta} = M_{tri(db)} + G_{meta(db)} \quad (23)$$

where $G_{meta(db)}$ is considered as 30, 20 and 10 dB for a low, medium and high loss environments respectively. We use a simulation based approach to analyze (23) to check the impact of various parameters such as antenna depth and orientation, operating frequency, number of coil turns and water conductivity etc. in the following section.

V. Simulation Results

We evaluate the performance in two different scenarios namely, lake water and seawater environments. The simulation pseudocode is mentioned in algorithm 1. Firstly, we will initialize the physical constants according to Fig. (4) and they are expressed as follows: the coil radius a is set to 0.05 m, the wire radius and conductivity are set to $r_w = 0.000255$ m and $\sigma_{coil} = 5.77 * 10^7\ S/m$ respectively. The permeability and conductivity of vacuum are μ_0 and ϵ_0. Then, the physical parameters for air are considered as $\mu_1 = \mu_0$, $\epsilon_1 = \epsilon_0$ and $k_1 = \omega\sqrt{\mu_1\epsilon_1}$. Similarly, the physical parameters for water are as follows: $\mu_2 = \mu_0$, $\epsilon_{r2} = 81\epsilon_0$, $\epsilon_2 = \epsilon_{r2} + j\frac{\sigma_2}{\omega}$ and $k_2 = \omega\sqrt{\mu_2\epsilon_2}$. Finally, the parameters for water floor are considered as $\mu_3 = \mu_0$, $\sigma_3 = 0.01$, $\epsilon_{r3} = 10\epsilon_0$, $\epsilon_3 = \epsilon_{r3} + j\frac{\sigma_3}{\omega}$ and finally $k_3 = \omega\sqrt{\mu_3\epsilon_3}$. After initializing the physical constants, we now generate two random orthogonal matrices each corresponding to the transmitter and the receiver's orientation as shown in Fig. (6). Here, each point in this generated grid corresponds to the TX and its corresponding RX point labeled above it. These are equivalent to the orientation matrices in equs. (18) and (19). Then, the LOS angle and the distance between the generated points are computed. Based on equs. (20) and (23), the magnetic field strength along the tri-directional coil and the metamaterial enhanced mutual induction are computed. Furthermore, the computed metamaterial enhanced mutual induction results are utilized to compute the power transfer efficiency derived in (17). The pseudocode can be repeated p times however, the results yielded will be quite similar given the generated random orientation matrices are analogous. To gain deeper insights into the derived expressions, we utilize the impact of five factors: LOS distance, depth of the transmitter, operating frequency, coil turns, and water conductivity.

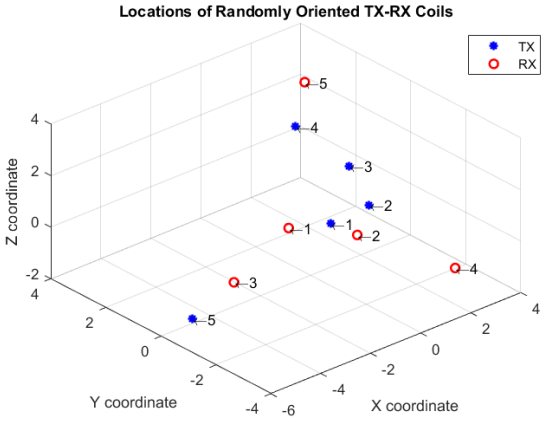

Fig. 6: Simulation of Random Orientation of TX-RX Pair

Algorithm 1 Power Transfer Efficiency Calculation

for $iter = 1 : p$ **do**
Ensure: Physical constants μ_1, ϵ_1 etc.
Initialize w, k, f etc.
while points == 2 **do**
get: p2p distance from grid
get: phase between points
create: random orthogonal matrices
verify: RR^T and TT^T == 1
verify: $R \cdot R$ and $T \cdot T$ == 0
Result: **T** and **R**
end while
while T and **R do**
compute $\mathbf{H}_{cl}(w,d)$
compute $\mathbf{M}_{meta}(w,d)$
end while
Require: V_S, R, L and C circuit parameters
compute $\eta = \frac{P_{R_L}}{P_{in}}$
RESULT: WPT Efficiency η
end for

A. Impact of Distance on Mutual Induction

We first analyze the impact of LOS distance between TX-RX on the metamaterial enhanced mutual induction. As seen

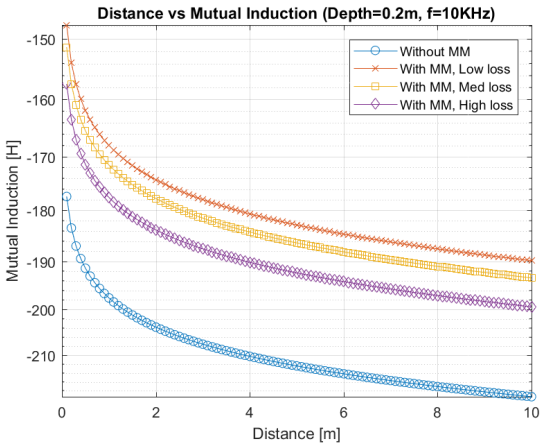

Fig. 7: Distance vs Mutual Induction

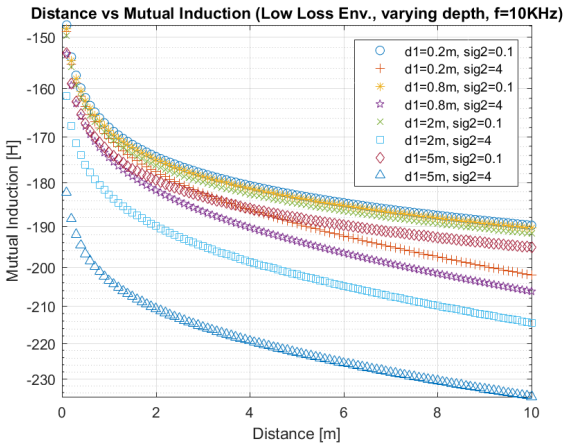

Fig. 8: Variation of Mutual Induction with varying depth, water conductivity in low loss environment

in Fig. (7), the depth is set to $d_1 = 0.2$ m, operating frequency is considered as 10 KHz. Intuitively, as the distance between the TX and RX increases, the mutual induction decreases. An important remark to note here is that, mutual induction gain with no metamaterial enhancement is significantly lower than the considered lossy mediums with metamaterial enhancement.

B. Impact of Depth and Water Conductivity on Mutual Induction in Lossy Environments

Here, we study the impact of the varying TX depth from water surface and simultaneously placing the coils in different water environments such as lake and sea water. As seen in Fig. (8), the operating frequency is set to 10 KHz in a low loss environment i.e; the metamaterial gain is 30 dB. The most promising results can be observed from a low depth-lake water environment. This is due to the impact of the lateral wave along the air-water interface which acts as a waveguide therefore, enhancing the mutual inductance. Counter intuitively, if we go deeper into the water, the gain diminishes as the effect of lateral wave decreases. Similarly, in Figs. (9) and (10), the simulations are repeated for a medium and high loss environment i.e.; 20 and 10 dB metamaterial gain respectively. As expected, the results are in accordance with the low loss environment. Additionally, the gain in mutual inductance is much lesser compared to the low loss case due to higher losses from the environment.

C. Impact of Frequency on Mutual Induction in Lossy Environments

Like the depth varying case, here we study the impact of varying operating frequency in different lossy environments. As seen in Figs. (11), (12) and (13) the operating frequency is changed from 10 KHz to 20 MHz in a low, medium and high loss environments respectively. The most promising results can be observed from the 10 KHz frequency.

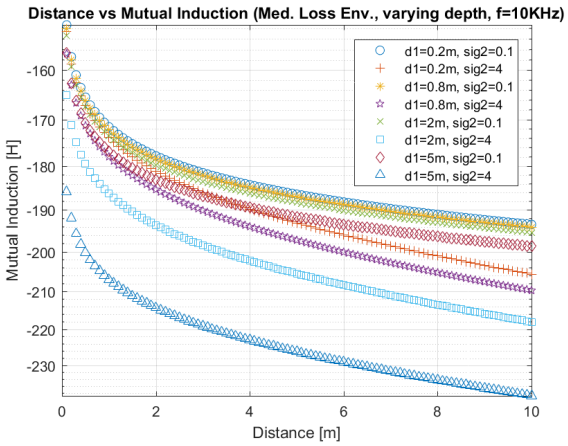

Fig. 9: Variation of Mutual Induction with varying depth, water conductivity in medium loss environment

D. Impact of Frequency on Wireless Power Transfer Efficiency

Up to this point, we investigated the important parameters that can affect the mutual induction, which couples the transmitting coil and the receiving coil. Next, we investigate the effect of different parameters on the wireless power transfer efficiency, namely, operating frequency, coil number of turns, coil orientation, and the distance. In Fig. (14), the impact of varying frequency is studied with respect to the wireless power transfer efficiency. The simulation settings are as follows: LOS distance between the TX-RX pair is set to 0.5 m and the depth of TX is set to 0.2 m from water surface. As expected, frequency is inversely proportional to mutual inductance. Thus, lower frequencies are desirable. Although the higher frequency can provide stronger coupling between the transmitting and receiving coils, the propagation loss is so high which prevents us from employing the frequency band.

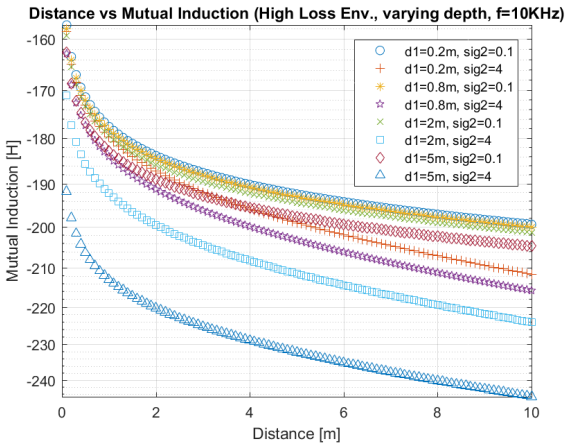

Fig. 10: Variation of Mutual Induction with varying depth, water conductivity in high loss environment

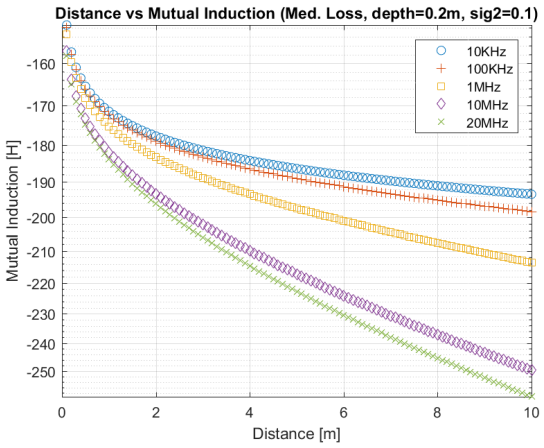

Fig. 12: Variation of Mutual Induction with varying frequency in medium loss environment

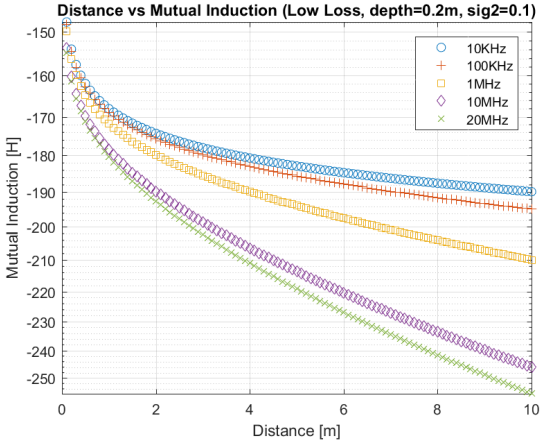

Fig. 11: Variation of Mutual Induction with varying frequency in low loss environment

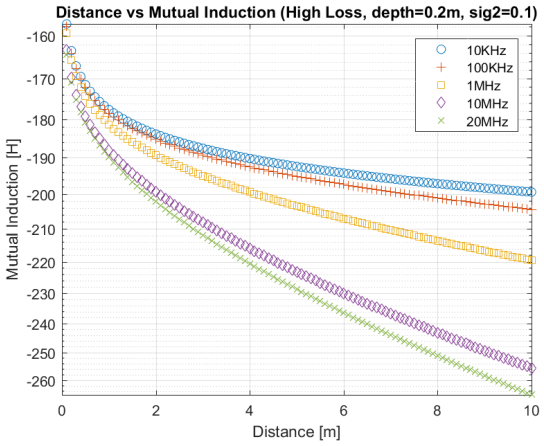

Fig. 13: Variation of Mutual Induction with varying frequency in high loss environment

E. Impact of Coil turns on Wireless Power Transfer Efficiency

In Fig. (15), impact of coil turns is presented in comparison to the wireless power transfer efficiency. The simulation settings are as follows: operating frequency is set to 10 KHz, LOS distance is set to 0.5m, depth is set to 0.5m and the conductivity of water is set to 0.1 S/m. As the number of coil turns increases, mutual inductance also increases. However, the gain diminishes if more coil turns are considered since the heat produced inside the coils increases the coil resistance.

F. Impact of Coil Orientation on Wireless Power Transfer Efficiency

In this paper, the tri-directional coil is employed thanks to its high reliability. In dynamic underwater environment, the AUV may change its orientation frequently, which creates significant polarization loss for the unidirectional coil. In this subsection, we numerically evaluate the reliability of the tri-directional coil in metamaterial shell. In Fig.16, the coil's orientation, i.e., θ and ϕ, varies from 0 to π, and 0 to 2π, respectively. In this way, it can cover all the directions in a spherical coordinates. We investigate the unidirectional coil to unidirectional coil communication and tri-directional coil to tri-directional coil communication. The transmitters' orientations are fixed and only the receivers' orientation vary. As shown in the figure, as the tri-directional coil's orientation changes, the wireless power transfer efficiency is nearly a constant, which shows its robustness to orientation change, while the wireless power transfer efficiency using unidirectional coil's changes dramatically since when the coils are well aligned the efficiency is high and when they are misaligned the efficiency drops significantly. As a result, the robust tri-directional coil with metamaterial shell is good candidate for wireless underwater charging.

G. Impact of Distance on Wireless Power Transfer Efficiency

In this final subsection, we study the impact of distance on wireless power transfer efficiency. As shown in Fig.17, the power efficiency decreases as the distance between the

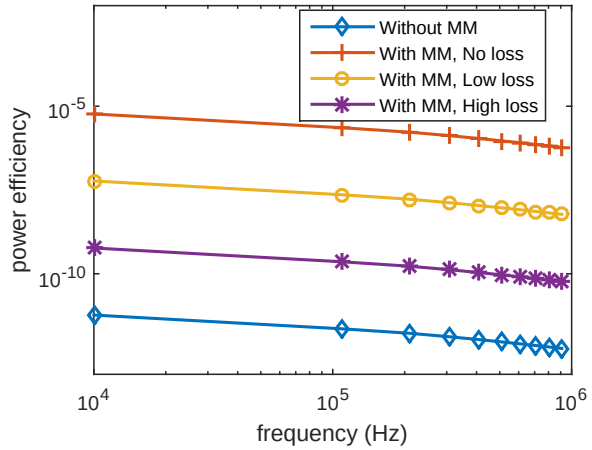

Fig. 14: Effect of frequency on wireless power transfer efficiency.

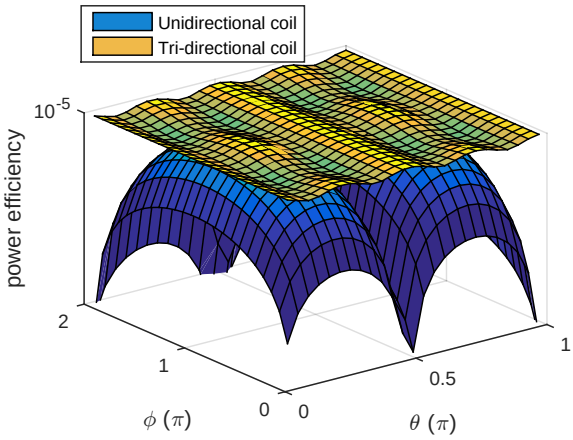

Fig. 16: Wireless power transfer efficiency using unidirectional coil and tri-directional coil

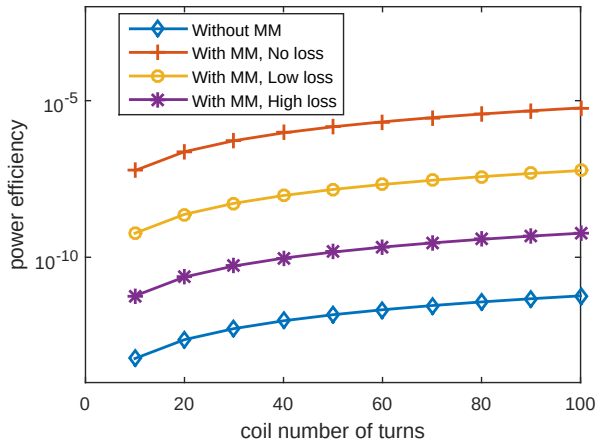

Fig. 15: Effect of coil turns on wireless power transfer efficiency.

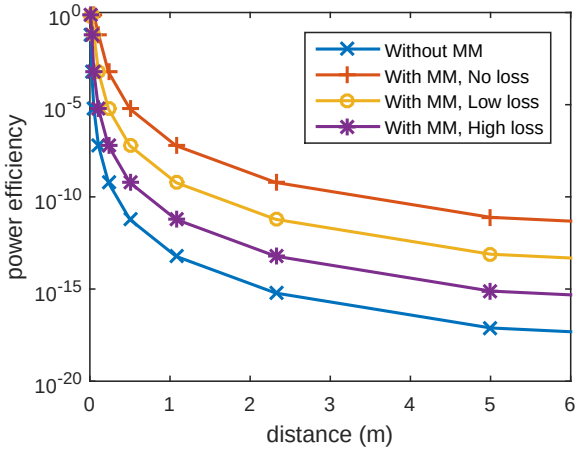

Fig. 17: Distance vs wireless power transfer efficiency using tri-directional antenna.

transmit-receive coils increases. The power transfer efficiency is higher than any other considered cases in a low loss environment. Another important observation is that the charging range for metamaterial enclosed antenna is higher than that of the antenna with no metamaterial shell. Additionally, we can also observe that in the vicinity of the transmitting antenna the power transfer efficiency is nearly 100%, especially the tri-directional coil with no loss metamaterial. This promising result suggests that the mobile vehicles in underwater environment can be directed to a mobile charging station and within reasonable distance, they can efficiently recharged.

VI. Conclusion

In this paper, the metamaterial enhanced tri-directional coil antenna was explored for an underwater wireless power transfer application. Simulation results indicate that the gain achieved by using a metamaterial shell significantly enhances the charging range and efficiency as compared to that of a conventional coil. It is also to be noted that, the impact of parameters such as LOS distance, operating frequency, antenna depth, coil turns, and water conductivity are very important to consider while designing the antenna for wireless power transfer. A low frequency, high coil turns construction of the antenna and low depth deployment of the antenna is preferable as the results indicate best performance in these settings.

References

[1] A. Vasilijevi, . Na, F. Mandi, N. Mikovi, and Z. Vuki, "Coordinated navigation of surface and underwater marine robotic vehicles for ocean sampling and environmental monitoring," *IEEE/ASME Transactions on Mechatronics*, vol. 22, no. 3, pp. 1174–1184, June 2017.

[2] R. Person, J. Blandin, J. M. Stout, P. Briole, V. Ballu, G. Etiope, G. Ferentinos, M. Masson, S. Smolders, and V. Lykousis, "Assem: a new concept of observatory applied to long term seabed monitoring of geohazards," in *Oceans 2003. Celebrating the Past ... Teaming Toward the Future (IEEE Cat. No.03CH37492)*, vol. 1, Sept 2003, pp. 86–90 Vol.1.

[3] E. M. H. Zahugi, M. M. Shanta, and T. V. Prasad, *Oil Spill Cleaning Up Using Swarm of Robots*. Berlin, Heidelberg: Springer Berlin Heidelberg, 2013, pp. 215–224. [Online]. Available: https://doi.org/10.1007/978-3-642-31600-5_22

[4] J. C. Kinsey, D. R. Yoerger, M. V. Jakuba, R. Camilli, C. R. Fisher, and C. R. German, "Assessing the deepwater horizon oil spill with the sentry autonomous underwater vehicle," in *2011 IEEE/RSJ International Conference on Intelligent Robots and Systems*, Sept 2011, pp. 261–267.

[5] M. J, V. A, A. VK, and M. Korulla, "Indigenous design and development of underwater wireless power transfer system," in *2016 Twenty Second National Conference on Communication (NCC)*, March 2016, pp. 1–6.

[6] K. Shizuno, S. Yoshida, M. Tanomura, and Y. Hama, "Long distance high efficient underwater wireless charging system using dielectric-assist antenna," in *2014 Oceans - St. John's*, Sept 2014, pp. 1–3.

[7] L. M. Pessoa, M. R. Pereira, H. M. Santos, and H. M. Salgado, "Simulation and experimental evaluation of a resonant magnetic wireless power transfer system for seawater operation," in *OCEANS 2016 - Shanghai*, April 2016, pp. 1–5.

[8] T. M. Hayslett, T. Orekan, and P. Zhang, "Underwater wireless power transfer for ocean system applications," in *OCEANS 2016 MTS/IEEE Monterey*, Sept 2016, pp. 1–6.

[9] A. Mittleider, B. Griffin, and C. Detweiler, *Experimental Analysis of a UAV-Based Wireless Power Transfer Localization System*. Cham: Springer International Publishing, 2016, pp. 357–371. [Online]. Available: https://doi.org/10.1007/978-3-319-23778-7_24

[10] B. Gulbahar and O. B. Akan, "A communication theoretical modeling and analysis of underwater magneto-inductive wireless channels," *IEEE Transactions on Wireless Communications*, vol. 11, no. 9, pp. 3326–3334, September 2012.

[11] C. Fang, X. Li, Z. Xie, J. Xu, and L. Xiao, "Design and optimization of an inductively coupled power transfer system for the underwater sensors of ocean buoys," *Energies*, vol. 10, no. 1, pp. 1–18, 2017. [Online]. Available: https://EconPapers.repec.org/RePEc:gam:jeners:v:10:y:2017:i:1:p:84-:d:87515

[12] H. Guo, Z. Sun, and C. Zhou, "Practical design and implementation of metamaterial-enhanced magnetic induction communication," *IEEE Access*, vol. PP, no. 99, pp. 1–1, 2017.

[13] H. Guo, Z. Sun, and P. Wang, "Multiple frequency band channel modeling and analysis for magnetic induction communication in practical underwater environments," *IEEE Transactions on Vehicular Technology*, vol. 66, no. 8, pp. 6619–6632, Aug 2017.

[14] H. Guo, Z. Sun, J. Sun, and N. M. Litchinitser, "M^2I: Channel modeling for metamaterial-enhanced magnetic induction communications," *IEEE Transactions on Antennas and Propagation*, vol. 63, no. 11, pp. 5072–5087, Nov 2015.